Title

Neurotoxicological effects induced by up-regulation of miR-137 following triclosan exposure to zebrafish (Danio rerio)

Authors

Liu, Jinfeng
Xiang, Chenyan
Huang, Wenhao
et al.

Publication Date

2019

DOI

10.1016/j.aquatox.2018.11.017

Peer reviewed

Aquatic Toxicology 206 (2019) 176–185

Contents lists available at ScienceDirect

Aquatic Toxicology

journal homepage: www.elsevier.com/locate/aqtox

Neurotoxicological effects induced by up-regulation of miR-137 following triclosan exposure to zebrafish (*Danio rerio*)

Jinfeng Liu[a], Chenyan Xiang[b,1], Wenhao Huang[a], Jingyi Mei[b], Limei Sun[a], Yuhang Ling[a], Caihong Wang[a], Xuedong Wang[b], Randy A. Dahlgren[c], Huili Wang[a,*]

[a] Zhejiang Provincial Key Laboratory of Medical Genetics, Key Laboratory of Laboratory Medicine, Ministry of Education, China, School of Laboratory Medicine and Life Sciences, Wenzhou Medical University, Wenzhou, Zhejiang, 325035, China

[b] National and Local Joint Engineering Laboratory of Municipal Sewage Resource Utilization Technology, Suzhou University of Science and Technology, Suzhou, 215009, China

[c] Department of Land, Air and Water Resources, University of California, Davis, CA95616, USA

ARTICLE INFO

Keywords:
Triclosan
Up-regulation miR-137
Regulatory target genes
Agomir and antagomir
Neurotoxic effect
Behavioral endpoint
Environmental toxicology

ABSTRACT

Triclosan (TCS) is a prevalent anthropogenic contaminant in aquatic environments and its chronic exposure can lead to a series of neurotoxic effects in zebrafish. Both qRT-PCR and W-ISH identified that TCS exposure resulted in significant up-regulation of miR-137, but downregulation of its regulatory genes (*bcl11aa*, *MAPK6* and *Runx1*). These target genes are mainly associated with neurodevelopment and the MAPK signaling pathway, and showed especially high expression in the brain. After overexpression or knockdown treatments by manual intervention of miR-137, a series of abnormalities were induced, such as ventricular abnormality, bent spine, yolk cyst, closure of swim sac and venous sinus hemorrhage. The most sensitive larval toxicological endpoint from intervened miR-137 expression was impairment of the central nervous system (CNS), ventricular abnormalities and notochord curvature. Microinjection of microRNA mimics or inhibitors of miR-137 both caused zebrafish malformations. The posterior lateral line neuromasts became obscured and decreased in number in intervened miR-137 groups and TCS-exposure groups. Up-regulation of miR-137 led to more severe neurotoxic effects than its down-regulation. Behavioral observations demonstrated that both TCS exposure and miR-137 over-expression led to inhibited hearing or vision sensitivity. HE staining indicated that hearing and vision abnormalities induced by long-term TCS exposure originated from CNS injury, such as reduced glial cells and loose and hollow fiber structures. The findings of this study enhance our mechanistic understanding of neurotoxicity in aquatic animals in response to TCS exposure. These observations provide theoretical guidance for development of early intervention treatments for nervous system diseases.

1. Introduction

Triclosan (5-chloro-[2,4-dichlorophenoxy] phenol, TCS) is a lipid-soluble, broad-spectrum antibacterial agent that is commonly added to a variety of personal care and industrial products, including hand soap, shampoo, toothpaste, and textile goods (Ying and Kookana, 2007). Due to its widespread use over the past 40 years, TCS has become a prevalent anthropogenic contaminant in aquatic environments worldwide. In recent years, TCS is frequently detected in the environment at ng/L to μg/L levels, leading to accumulation in aquatic biota and humans (Wang and Tian, 2015; Meador et al., 2018). Wastewater treatment plant influent concentrations of TCS have been reported to reach levels as high as 86.2 μg/L (Kumar et al., 2010). For example, raw influent TCS concentrations ranged from 3000 to 14,000 ng/L, whereas effluent concentrations ranged from 161 to 462 ng/L in Red River basin wastewater/sewage treatment plants (Weilin et al., 2007). The presence of antimicrobial agents in the environment, even at low concentrations, may be hazardous because of its potential for bioaccumulation within the aquatic food web. Accumulation of TCS in aquatic organisms, such as shellfish, fish and marine mammals, is well-established (Ruszkiewicz et al., 2017).

In zebrafish (*Danio rerio*) embryos, TCS exposure delayed development of secondary motor neurons at concentrations from 550 to 1600 μg/L (Muth-Köhne et al., 2012). Further, TCS-induced edema reduced blood circulation and produced malformations of the head, heart and tail in embryos (Muth-Köhne et al., 2012). It was reported that TCS induced apoptosis in mice neuronal cells and pro-apoptotic effects in rat neural stem cells

* Corresponding author.
E-mail addresses: 964781955@qq.com (C. Xiang), whuili@163.com (H. Wang).
[1] Co-first author.

https://doi.org/10.1016/j.aquatox.2018.11.017
Received 13 August 2018; Received in revised form 18 November 2018; Accepted 19 November 2018
Available online 22 November 2018
0166-445X/

(Szychowski et al., 2016; Kyung et al., 2016). Previous literature indicated that prenatal TCS exposure was associated with reduced head circumference at birth in human boys (Lassen et al., 2016; Philippat et al., 2014). This discovery raises concerns over the role of TCS in neurodevelopment, since reduced head circumference at birth has been linked to impaired cognitive performance later in life (Veena et al., 2010). TCS can impair excitation-contraction coupling and Ca^{2+} dynamics in striated muscle and disrupt mitochondrial structure, thereby having a severe effect on molluscan neurons (Cherednichenko et al., 2012; Popova et al., 2018; Weatherly et al., 2018). Elevated urinary TCS concentrations at birth were associated with significantly lower cognitive test scores at an age of 8 yrs (Jackson-Browne et al., 2018). Ruszkiewicz et al. (2017) reported that TCS might exert adverse effects on central nervous system (CNS) functions, mainly through induction of apoptosis and oxidative stress. These reports attest to potentially deleterious effects of TCS on the CNS. TCS can be detected in the hypothalamus mitochondrial structure, indicating its ability to infiltrate and potential to accumulate in the brain region responsible for the regulation of metabolism, it can cross the blood brain barrier (Van et al., 2017). Nevertheless, there is a paucity of data regarding the specific microRNAs (miRNAs) induced by TCS exposure.

miRNAs are small non-coding regulatory RNAs that have been highly conserved in evolution. They post-transcriptionally regulate gene expression by inducing cleavage of their target mRNAs, inhibiting their translation or causing degradation of the target messenger RNAs (Carthew and Sontheimer, 2009; Yu and Pan, 2012). miRNAs play an important role in the process of development, differentiation, cell proliferation and apoptosis, hormone secretion, tumor formation and neurodegenerative diseases. They are critical to neurodevelopment and adult neuronal processes by modulating the activity of multiple genes within biological networks (Krol et al., 2010; Xu et al., 2017).

miR-137, as a brain-enriched microRNA, plays an important role in regulating embryonic neural stem cells (NSCs) fate determination, neuronal proliferation and differentiation, and synaptic maturation. Its dysregulation causes changes in the gene expression regulation network of the nervous system, thus inducing mental disorders in humans, including schizophrenia susceptibility (Yin et al., 2014). miR-137 negatively regulates dopamine transporter expression and functions in neural cells. It can inhibit Parkin-induced autophagy, and the increase of miR-137 expression leads to decreased autophagy, which is an inducer of Parkinson's disease (Jia et al., 2016). Overexpression of miR-137 in the brain improves behavioral changes in post-stroke depression rats by suppressing target gene expression at the post-transcriptional level (Zhao et al., 2013). Siegert et al. (2015) reported a new mechanism of synaptic modulation that may be perturbed in disorders such as schizophrenia, and this mechanism involved *in vitro* and *in vivo* miR-137 gain of function downregulation for three presynaptic target genes that caused impairment in synaptic vesicle trafficking and alterations in synaptic plasticity (Siegert et al., 2015). Additionally, several studies demonstrated that miR-137 was related to neurotoxicity and nerve injury in mice and human cell lines (He et al., 2017; Gao et al., 2017).

To expand beyond the findings of the previous literature, the primary objective of this study was to probe mechanisms associated with TCS-induced miR-137 expression in zebrafish. The effect of miR-137 abnormal expression on neurodevelopment was rigorously investigated using manual intervention, behavioral analysis, morphological observations and neuromast hair cell staining. The findings of this study advance our understanding of neurotoxicity in aquatic animals resulting from TCS exposure, and provide theoretical guidance for development of early intervention treatments for the drug-induced abnormal neurodevelopment in mammals.

2. Material and methods

2.1. Ethics statement

The Institutional Animal Care and Use Committee (IACUC) at Wenzhou Medical University approved our study plan for ethical use of zebrafish (*Danio rerio*). All studies were carried out in strict accordance with IACUC guidelines. All zebrafish surgery was performed on ice to decrease suffering.

2.2. Chemicals

TCS (5-chloro-2-[2,4-dichlorophenoxy]phenol) was purchased from Sigma-Aldrich (St. Louis, USA; CAS No. 3380-34-5, 99.9% purity). Acetone was obtained from Sinopharm Chemical Reagent Co. (Shanghai, China). Formamide (CAS No.75-12-7, purity ≥ 99%) was acquired from Aladdin (Shanghai, China).

2.3. Zebrafish maintenance and exposure protocols

Wild-type (AB strain) zebrafish were raised in dechlorinated and filtered water at 28°C with a 14-h light:10-h dark cycle photoperiod (light on at 8 a.m.). Zebrafish maintenance followed Westerfield (2000). A series of TCS-exposure concentrations was chosen according to its LC_{50} and EC_{50} values (Zhang et al., 2018; Oliveira et al., 2009), environmentally relevant concentrations, and preliminary experimental results. The data of death/malformation recorded/collected rates and malformed zebrafish information were reported in our previous study, and the LC_{50} and EC_{50} values of TCS for 120-hpf zebrafish were 510 and 360 μg/L (Zhang et al., 2018). In Oliviera's study, TCS showed acute toxicity for embryos and larvae with a 96 hpf LC_{50} of 420 μg/L (Oliveira et al., 2009). Embryos were exposed to a series of TCS concentrations (0, 62.5, 125 and 250 μg/L (equivalent to 0, 0.22, 0.43 and 0.86 μmol/L, respectively). Low-dose TCS concentrations (0, 40, 80 and 160 μg/L (equivalent to 0, 0.14,0.27 and 0.56 μmol/L, respectively) were chosen for zebrafish continuous exposure studies from the embryo (6 hpf, hours post-fertilization) to adult (90 dpf, days post-fertilization) growth stages. Control embryos were treated with 0.0025% acetone (as referenced to the highest 250 μg/L TCS-exposure treatment). These TCS-exposure concentrations simulate real-world environmental levels in human-impacted aquatic ecosystems. Prior to locomotor behavioral test, larvae were evaluated using a microscope and any dead or malformed individuals were excluded. The TCS-exposure solutions were renewed daily to maintain stable water quality and TCS concentration.

2.4. Target genes prediction and expression analyses of miR-137 using qRT-PCR and WISH

Two miRNA target databases were used to predict the target genes of miR-137: TargetScan (http://www.targetscan.org/) and Diana Tools (http://diana.imis.athena-innovation. gr/DianaTools/index.php?r = microT_CDS/index). For functional annotation of the genes targeted by the miRNAs, Kyoto Encyclopedia of Genes and Genomes (KEGG) functional classification (http://www.genome.jp/kegg/) was performed using the web-based tool, Database for Annotation, Visualization and Integrated Discovery (DAVID, http://david.abcc.ncifcrf.gov/) (Huang et al., 2009). Sequence homology comparison among different species was conducted using the rVista 2.0 database (https://rvista.dcode.org/), and Diana miRPath V3 software (http://snf-515788.vm.okeanos.grnet.gr/) was used to produce heatmaps of miR-137 expression.

To determine miR-137 expression at the transcriptional level *in vivo*, qRT-PCR and W-ISH were performed. We used the All-in-One™ miRNA qRT detection system (Genecopoeia; Rockville, USA) followed by SYBR Green PCR analysis (Bio-Rad; Hercules, USA) to confirm and measure significant differentially expressed miRNAs. Total RNA from 96 homogenized larval zebrafish for each replicate of TCS-exposure treatments (0, 62.5, 125 and 250 μg/L) from 6 to 120 hpf was isolated using TRIzol regent with U6 as the endogenous reference (Table S2). Primers were designed and synthesized by Sangon Biotech (Shanghai, China). The cDNA probes for miR-137 were synthesized by Sangon Biotech (Shanghai, China) and labeled with digoxigenin (DIG). Embryos in each treatment groups were treated with 0.5% N-

phenylthiourea (PTU; Aladdin, Shanghai, China) and collected in 1.5 mL RNase-free EP tubes, each tube containing 15 embryos. Whole-mount ISH was performed following Thisse and Thisse (2008).

2.5. Microinjection and phenotype observation

Adult zebrafish were mated and spawned for 10 ~ 15 min, and the fertilized eggs were quickly collected for microinjection. MicroRNA mimics and inhibitors for miR-137 were synthesized by GenePharma (Shanghai, China) and used as received. The concentration of mimic or inhibitor solutions was adjusted to 200 μg/mL; aliquots (2 nL) of the solution were injected into each egg (Pli-100 A, Warner Instruments, Hamden, USA), and any dead embryos were removed after 12 h.

Thirty embryos or larvae in each treatment were randomly selected and anesthetized with 0.03% tricaine (buffered MS-222; Sigma, St. Louis, USA) for 30 s, then carefully observed and photographed using an optical microscope (DM2700 M, Leica, Heidelberg, Germany).

2.6. Live larvae staining using FM 1-43 dye

Experimental zebrafish were washed three times in EM solution for 5 min before staining. Live larvae were exposed to a solution of 2 IM FM™ 1-43 Dye (*N*-(3-triethyl-ammonium propyl)-4-(4-(dibutylamino) styryl) pyridinium dibromide (GeneBio; Shanghai, China), which was diluted in EM solution for 2 min in the dark. Larvae were then rinsed in EM solution three times for 30 s in each wash and then anaesthetized in MS-222. Samples were immediately imaged using a SZX16 Olympus microscope (Tokyo, Japan).

2.7. Behavioral assessment

To examine larval responses to external stimuli and autonomous movement (without any stimuli), 120-hpf larvae in control and treatment groups were transferred to 96-square-well plates. We used one larva for each well and each plate included one control and two treatment groups; there were 24 larvae for each group and three replications for each plates giving a total of 72 larvae used as biological replicates for each treatment. Plates were placed in a DanioVision Observation Chamber (Noldus IT, Wageningen, Netherlands) for a 5-min adaption before initiating a tapping or light stimulation (Tapping intensity level = 4; Light = 100%). Video was collected and analyzed to compute the mean swim speed in the 5 min following stimulation using EthoVision XT software (Noldus IT, Wageningen, Netherlands).

2.8. Histopathological observations

To explore whether TCS exposure induced histopathological injury to the CNS, 90-dpf F0-zebrafish brain and spinal cord were observed by means of haematoxylin and eosin (H&E) staining. Staining was conducted following manufacturer's instructions for the Hematoxylin-Eosin/HE® Staining Kit (Solarbio, China). Each experiment included 3 biological replicates and 3 technical replicates for each biological replicate. The tissue structure was observed by optical microscopy (DM2700 M, Leica Germany).

2.9. Statistical analysis

Experimental data were reported as mean ± SD (standard deviation; the biological and technical replicates for each test are listed in Table S3). When homogeneity of variance assumptions were satisfied, one-way analysis of variance (ANOVA) was used to assess TCS-exposure effects, followed by post-hoc Tukey tests for multiple mean comparisons among different experimental groups. All statistical analyses were conducted with SPSS 18.0 (SPSS, Chicago, USA) using significance levels of $p < 0.05$ (*), $p < 0.01$(**) or $p < 0.001$(***).

3. Results

3.1. Bioinformatics and expression analyses of differentially expressed miRNAs following TCS exposure

The miRNA expression patterns are remarkably specific and diverse, suggesting that expression sites and distribution of miRNAs in different tissues and organs are strongly related to their functions (Kloosterman et al., 2006). Based on previous literature, five miRNAs (miR-137, miR-181a, miR-181b, miR-128 and miR-100) were chosen for investigation due to their expressions in zebrafish CNS during embryonic development (Wienholds et al., 2005; http://www.microrna.org/microrna/%20getExprData.do). qRT-PCR was conducted to determine the expressions of the five miRNAs following TCS exposure from 6 to 120 hpf. Among these miRNAs, significant up-regulation ($p < 0.01$) was observed for miR-137 (Fig. 1B). As a brain-enriched miRNA, miR-137 plays an important role in regulating embryonic neural stem cells (NSCs) fate determination, neuronal proliferation and differentiation, and synaptic maturation (Yin et al., 2014).

To better understand the biological functions of the five miRNAs, we predicted their potential target genes using TargetScan software. According to the principles of lowest energy and highest score value in the TargetScan database, we analyzed 3′-UTR binding information for the screened target genes of the five miRNAs. A total of 4567 genes were predicted as target genes of miR-137, among which 364 were also predicted in Diana Tools (Threshold = 0.7). Among coexistence genes, two target genes *bcl11aa* and *Runx1* were determined to have low-binding free energy to 3′-UTR and a high total context + score (Fig. 1C). Target gene functions regulated by dre-miR-137 and signaling pathway information are summarized in Table S1.

Pathway enrichment analysis was used to determine functional associations of miR-137, miR-181a, miR-181b, miR-128, miR-100 in humans (Fig. 1D) and mice (Fig. 1E) using DIANA miRPath V3 software. In humans, hsa-miR-137 mainly participates in the ERbB signaling pathway; in mice, mmu-miR-137 is mainly associated with MAPK signaling pathway, ECM-receptor interaction, thyroid hormone signaling pathway and oxytocin signaling pathway. Notably, there is currently a lack of information on dre-miR-137 function in zebrafish. The MAPK signaling pathway is reported to play an important role in pathogenesis of neurodegenerative diseases, such as Alzheimer and Parkinson disease (Mufson et al., 2012). The miR-137 entity was highly conserved in terms of their sequences in zebrafish, humans, mice, rats and chickens. Analysis of sequence homology was conducted for zebrafish and mice using the human sequence as a reference. miR-137 had high sequence homology in zebrafish, mice and humans (Fig. 1E, F), and thus was chosen for more detailed investigation.

3.2. qRT-PCR and W-ISH analysis of miR-137 expression following TCS exposure

The expression change of miR-137, using the U6 signal as a stable reference gene, was used to determine the effect of TCS exposure on 120-hpf zebrafish. qRT-PCR and W-ISH results showed that the 125 and 250 μg/L TCS-exposure treatments significantly increased miR-137 expression ($p < 0.01$) compared to the control group. In the absence of TCS exposure, miR-137 showed elevated expression in the forebrain and olfactory bulb. Following TCS exposure, miR-137 was mainly expressed in the visceral mass along with the forebrain and olfactory bulb. TCS exposure resulted in significant up-regulation of miR-137 ($p < 0.05$ or $p < 0.01$) and showed an obvious concentration-dependent relationship, especially in the olfactory bulb and visceral mass (Figs. 2A and S1).

The olfactory bulb is the main sensory organ of the olfactory system (Friedrich, 2013). The olfactory system is responsible for collecting and processing long distance chemical information and participating in zebrafish behavioral activities, such as foraging, courtship, escape and migration. Similarly, the expression of miR-137 by W-ISH demonstrated

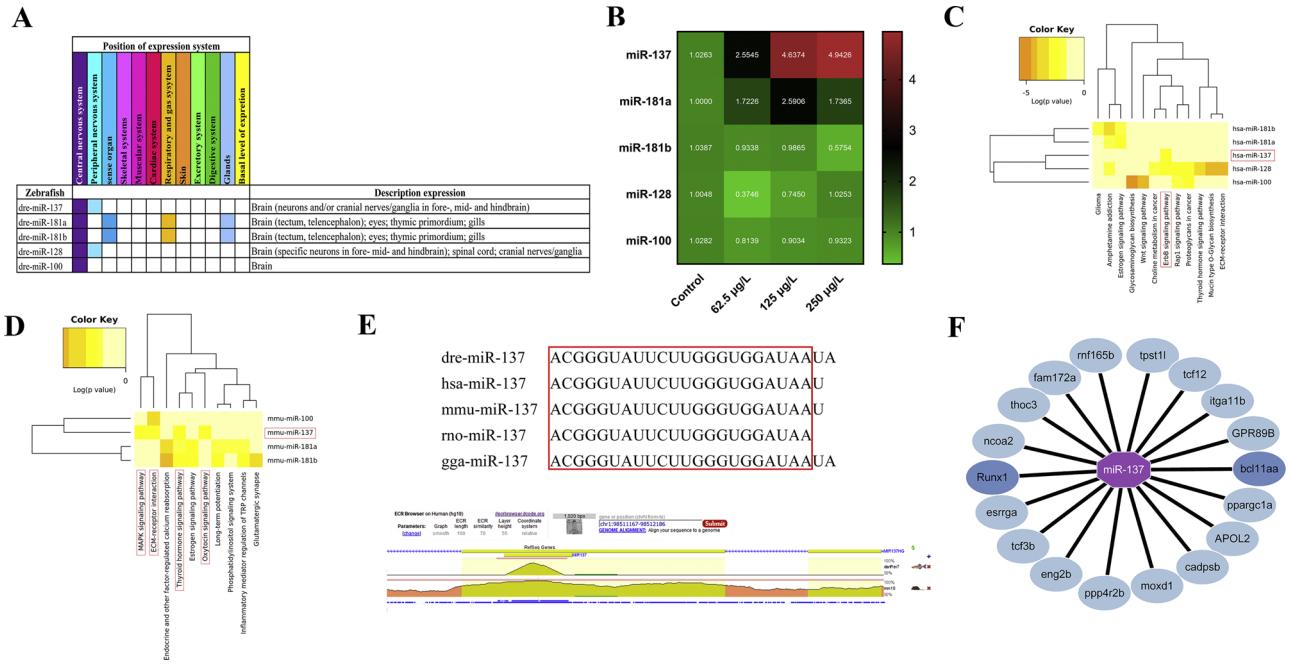

Fig. 1. The miR-137 sequence homology and its target gene-concerned pathways. (A) The main expression system of five miRNAs in zebrafish; (B) Clustering analyses of five miRNAs by qRT-PCR in 120-hpf larvae; (C) Prediction using human miRNAs (p-value threshold < 0.05 and MicroT threshold < 0.08); (D) Prediction using mice miRNAs (p-value threshold < 0.05 and MicroT threshold < 0.08); (E) Evolutionary conservation of miR-137 sequence and the same cluster in zebrafish, humans, rats, mice and chickens; (F) Related target genes of miR-137. The network diagram in Fig. 1F is plotted by Cytoscape (v3.6) software; Heatmap of miRNAs *vs.* pathways, miRNAs are clustered together by exhibiting similar pathway targeting patterns, and pathways are clustered together by related miRNAs.

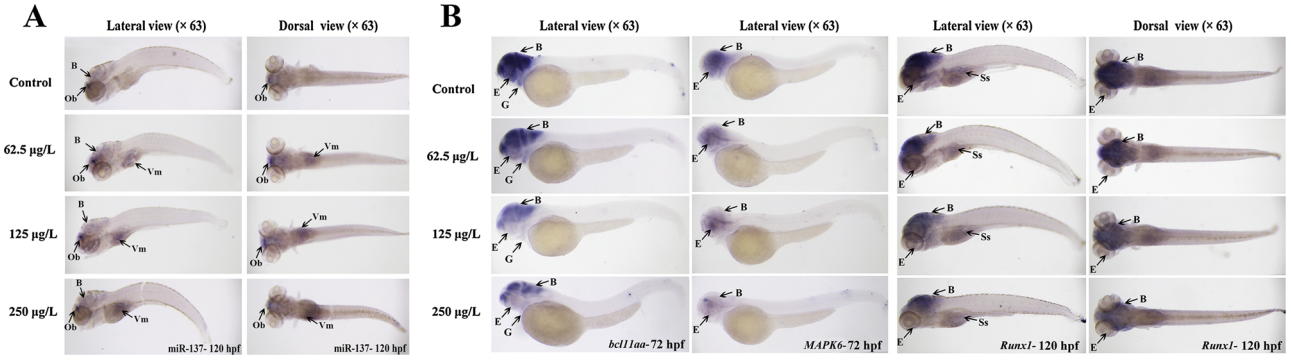

Fig. 2. miR-137 and its target gene expression after TCS exposure by W-ISH. (A) W-ISH of miR-137 in 120-hpf larvae; (B) W-ISH of miR-137 target and regulatory genes in 72 or 120-hpf larvae. A and B show the expression of hybridization signals by lateral and dorsal view in control and treatment groups; Abbreviations in Fig. 2A and B: B, brain; E, eye; G, gills; Ob, olfactory bulb; Vm, visceral mass.

a positive TCS concentration-dependent relationship, i.e., increasing expression with an increase in TCS-exposure concentration (Fig. 2A). A comparable trend was also observed for miR-137 expression by qRT-PCR, especially in the 125 and 250 μg/L treatments (Fig. S1). Overall, the W-ISH and qRT-PCR results examining changes in miR-137 expression were in general agreement (Fig. 1B).

3.3. W-ISH analysis of miR-137 target gene expression following TCS exposure

Based on bioinformatics analysis, miR-137 was mainly associated with the ERbB signaling pathway in humans and MAPK signaling pathway in mice, but there is a lack of information concerning the dre-miR-137 signaling pathway in zebrafish. To further explore the neuro-related regulatory mechanisms and functions of miR-137, expression sites and changing patterns for the two neurodevelopment-related target genes (*bcl11aa* and *Runx1*) and MAPK signaling pathway-related gene (*MAPK6*) were determined by W-ISH. In the control group, both *bcl11aa* and *MAPK6* showed high expression in the CNS. *bcl11aa* is closely related to lymphocyte development, proliferation, differentiation and tumorigenesis (He et al., 2014; Eberle et al., 2011). *bcl11aa* was mainly distributed in the brain, including forebrain, midbrain and hindbrain, and gill of 72-hpf larval zebrafish and displayed a significant decrease in TCS treatments compared to the control group ($p < 0.01$ or $p < 0.001$). At high TCS concentrations (125 and 250 μg/L), *bcl11aa* was negligibly expressed in gill and slightly expressed in the brain (forebrain, midbrain and hindbrain).

MAPK6 encodes the Ser/Thr protein kinase family member MAPK6, which is closely related to mitogen-activated protein kinases (Hoeflich et al., 2006). It was mainly expressed in the brain (forebrain and midbrain) of 72-hpf larval zebrafish with a significant decrease ($p < 0.01$) in TCS-exposed groups compared to the control group. In the 250 μg/L treatment, *MAPK6* expression was significantly decreased after TCS exposure ($p < 0.001$), with low levels in the forebrain and negligible expression in the midbrain (Fig. 2C and B-c). *Runx1* may positively regulate the ErbB/HER2 signaling pathway, which was the only target gene-concerned pathway of hsa-miR-137. It has been reported to modulate SOS1 expression in gastric cancer cells (Mitsuda

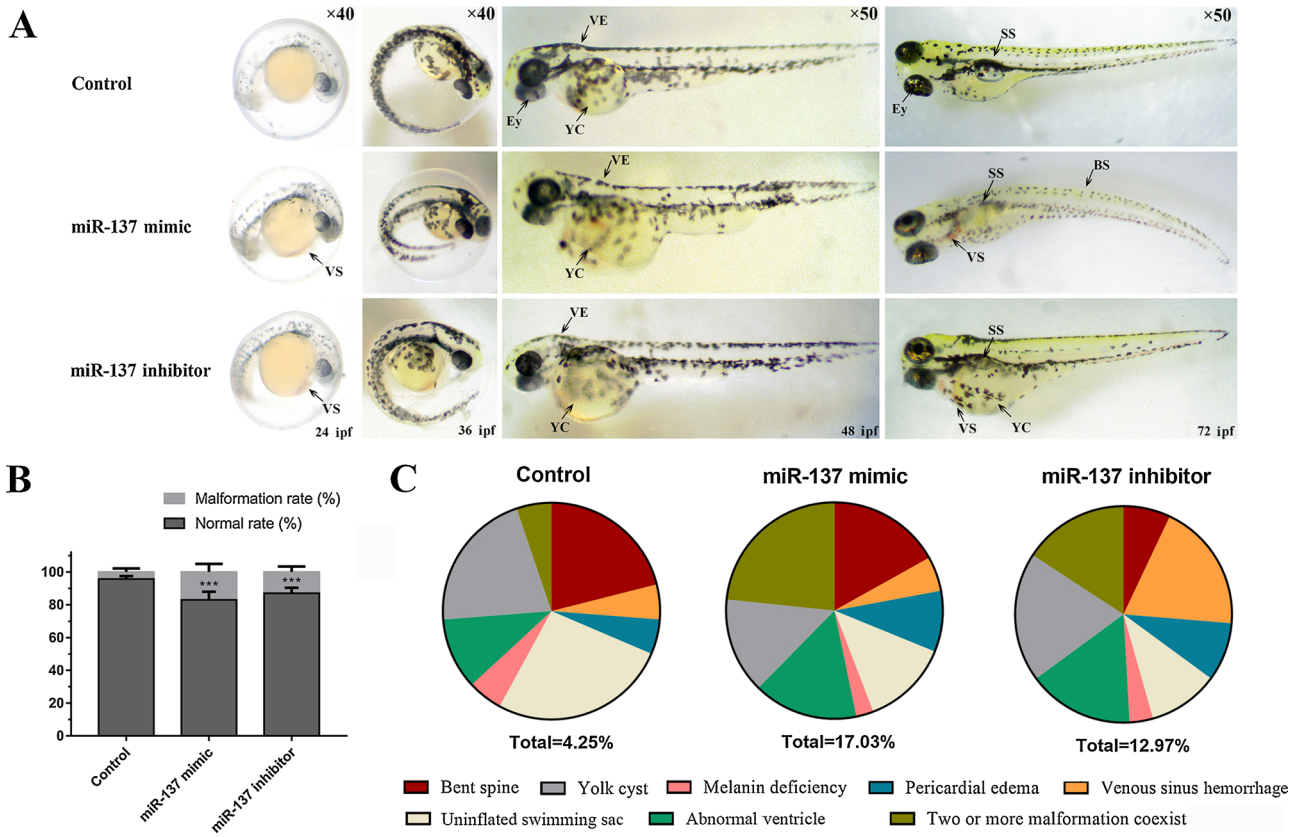

Fig. 3. Zebrafish malformation after microinjection of miR-137. (A) Zebrafish malformation observation after microinjection from 24 to 72 ipf after microinjection; (B) Statistical analysis of malformation rate at 72 ipf larvae. (C) Statistical analysis of different malformation patterns ratio. VS, venous sinus; YC, yolk cyst; VE, ventricle eminence; SS, swimming sac; BS, bent spine;"***" indicate significance at $p < 0.001$.

et al., 2018) and may promote proliferation and neuronal differentiation in adult mouse neurosphere cultures (Logan et al., 2015). *Runx1* hybridization signals were not observed in the 72-hpf and 120-hpf zebrafish, but they displayed prominent changes in the brain (forebrain, midbrain and hindbrain) and swimming sac. *bcl11aa*, *MAPK6* and *Runx1* were down-regulated with increasing TCS concentrations (Fig. 2C and B). As described above, qRT-PCR and W-ISH analyses demonstrated that miR-137 expression showed a positive TCS concentration-dependence, but expression of its three target genes (*bcl11aa*, *MAPK6* and *Runx1*) displayed a negative TCS concentration-dependence. Thus, an inverse expression pattern was observed between miR-137 and its regulatory genes.

3.4. Effect of intervened miR-137 expression on development of larval zebrafish

Our previous study demonstrated that TCS and its derivatives could reduce blood circulation and produce a series of malformation symptoms in the head, heart and tail (Zhang et al., 2018). In this study, expressions of miR-137 target genes were affected by TCS exposure. Therefore, we characterized the regulatory role of miR-137 in the nervous system using qRT-PCR analysis. Lateral-line neuromast staining, behavioral analysis and W-ISH were also conducted in zebrafish larvae by means of injecting miR-137 agomir for over-expression and antagomir for suppression.

The sequences of agomir and antagomir for miR-137 were synthesized and injected into zebrafishI-cell embryos (2 nL of 200 ng/μL for each embryo). Obvious toxicological effects or phenotypic malformation occurred in the intervened miR-137 groups compared to the control group. At different developmental stages after intervention (24–72 ipf), the intervened miR-137 led to a series of abnormalities, such as ventricular abnormality, bent spine, yolk cyst, closure of swim sac and venous sinus hemorrhage (Fig. 3A). The most sensitive larval toxicological endpoint of intervened miR-137 expression was impairment of the CNS, leading to ventricular abnormalities and curvature of the notochord. The miR-137 mimic group displayed more linear ventricle, bent spine and coexistence of multiple malformations compared to the inhibitor group. As a result, we conclude that up-regulation of miR-137 led to more severe neurotoxic effects than down-regulation (Fig. 3C).

3.5. Effects of TCS and intervened miR-137 expression on lateral-line neuromast

The zebrafish lateral line system is an important sensory organ derived from the skin and contributes to feeling functions of water flow, water pressure, water temperature and hearing via converting external acoustic signals into neural electrical stimulation in the brain. Therefore, it plays an important role in training, predation and direction discrimination Damblychaudière et al. (2003). The neuromast is the basic unit of the lateral-line system, which is distributed in the head, trunk and tail (Fig. 4A) and has a fixed pattern in its development (Hamilton et al., 2014). Thus, it is an excellent model to study the development, regeneration and apoptosis of hair cells. Through FM™1–43dye staining, the neuromasts in the control group were observed to be orderly arranged in the lateral line. Up-regulation of miR-137 led to similar pathological changes as induced by TCS exposure (Fig. 4B–D). In the negative control group, neuromasts were clearly visible and distributed throughout the trunk in an orderly pattern. In contrast, the posterior lateral line neuromasts in the miR-137 mimic group became obscured and decreased in number ($p < 0.05$). The trunk and terminal neuromasts changed in quantity and distribution following exposure to high TCS concentrations (250 μg/L) or agomir-

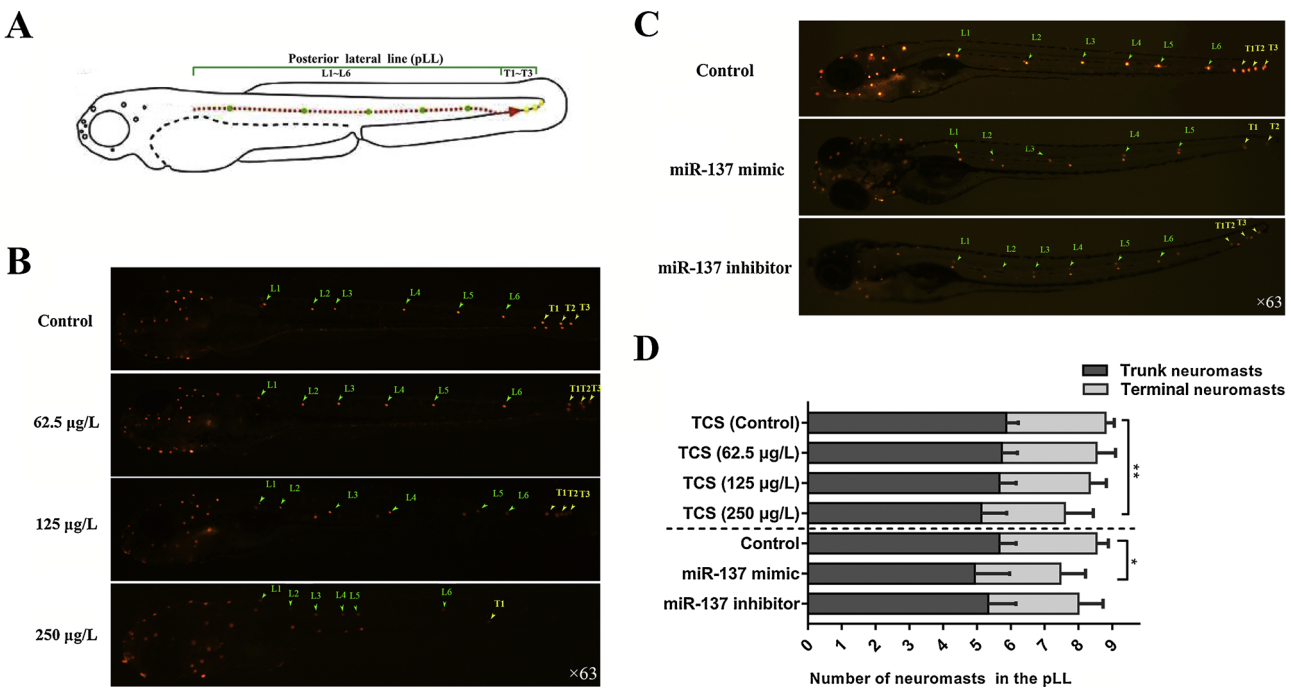

Fig. 4. Lateral-line neuromast staining on 120-hpf zebrafish after TCS exposure and microinjection of miR-137 by FM 1–43. (A) Lateral-line system pattern in normally developed zebrafish; (B) Neuromast staining after TCS-exposure; (C) Neuromast staining after microinjection of miR-137; (D) Number of neuromasts in the pLL. "L1-L6" represents the trunk neuromast on one side of the larval zebrafish; "T1-T3" represents the terminal neuromast on one side of the zebrafish larval; the green arrows point to each trunk neuromast and the yellow arrows point to the terminal neuromast formed in the tail; The ex/em wavelengths were 510/625 nm (in MeOH) and 480/598 nm (in membranes).

137 injection. In the miR-137 inhibitor group, lateral line neuromasts became obscured, but were less severely impacts compared to the mimic group (Fig. 4C and D). These results demonstrated that zebrafish lateral-line neuromast development was very sensitive to TCS-exposure concentration and miR-137 expression.

3.6. Effects of miR-137 abnormal expression on zebrafish behavior

Stress responses of zebrafish larvae to an external acoustic or optical stimulus are often used as evaluation criteria for normal/abnormal development of hearing and vision. The average swim speed after stimulation was adopted as a response metric. After continuous TCS exposure to 120-hpf larval zebrafish, no significant difference in spontaneous swim speed was observed in the 62.5 μg/L treatment, but swim speed significantly decreased in the 125 and 250 μg/L treatments ($p < 0.001$), suggesting that high TCS-exposure concentrations decreased locomotor activity (Fig. 5A). The intervened miR-137 also led to a significantly decreased swim speed for the 120-hpf zebrafish larvae ($p < 0.01$ or $p < 0.001$), especially for the miR-137 over-expression group ($p < 0.001$; Fig. 5D). Larval light-stimulation tests showed a quick response (within 1 min) in the control group, but a delayed, startled response for 120-hpf larvae exposed to TCS. A relatively high swimming speed appeared after 4–6 min of light stimulation in the 62.5, 125 and 250 μg/L treatments compared to 3 min in the control group. These observations suggest that zebrafish sensitivity to light stimulation was inhibited by TCS exposure (Fig. 5B). In the over-expression miR-137 group, a weak startled response was observed (Fig. 5E) and locomotor activity was relatively low in the light stimulation tests. In the tapping stimulation tests, an intense and quick response was observed in the control group. After TCS exposure to 120-hpf larvae, intensity of the startled response decreased in the 62.5 μg/L treatment. In comparison, the startled response was delayed and displayed a decreased intensity in the 125 and 250 μg/L treatments (Fig. 5E), showing an insensitive response to sound stimulation (Fig. 5E). In the miR-137 mimic group, a relatively high locomotor speed appeared in 5 min, which was delayed approximately 2 min compared to the control group. These observations demonstrate that TCS exposure and miR-137 over-expression led to impaired hearing or vision sensitivity, showing an impeded response to acoustic or optical stimulation.

3.7. W-ISH analysis for target gene expression of miR-137 after microinjection

qRT-PCR results showed that agomir significantly increased miR-137 expression by ca. 3.5-fold ($p < 0.05$; Fig. 6A). In contrast, antagomir slightly decreased miR-137 expression compared with the control group. These findings demonstrate that miR-137 agomir causes over-expression of mature miR-137 (Fig. 6A).

In the control group, *bcl11aa*, *MAPK6* and *Runx1* showed high expression in the brain. *bcl11aa* was mainly expressed in the brain and gill of 72-hpf larvae; however, it showed a significant decrease in the miR-137 over-expression group. A contrasting trend was observed in the miR-137 knock-down group, especially in the hindbrain. *MAPK6* was mainly expressed in the forebrain and midbrain of 72-hpf larvae; however, its expression was observed at a lower level in the miR-137 mimic group than in the control group. Through the integral optical density (IOD) analysis of miR-137 target and regulatory genes, *Runx1* expression was observed to be prominently changed in the brain and swimming sac, showing a similar gene expression trends as other genes (*bcl11aa*, *MAPK6*). All three genes were down-regulated after over-expression of miR-137 (Fig. 6B and C). These results showed that TCS exposure led to up-regulation of miR-137 causing abnormal expression of its target genes and a series of neurotoxic effects.

3.8. Histopathological observations of brain and spinal cord tissues following TCS exposure

HE staining was conducted to investigate chronic CNS injury induced by long-term exposure to low-doses of TCS. HE staining of adult

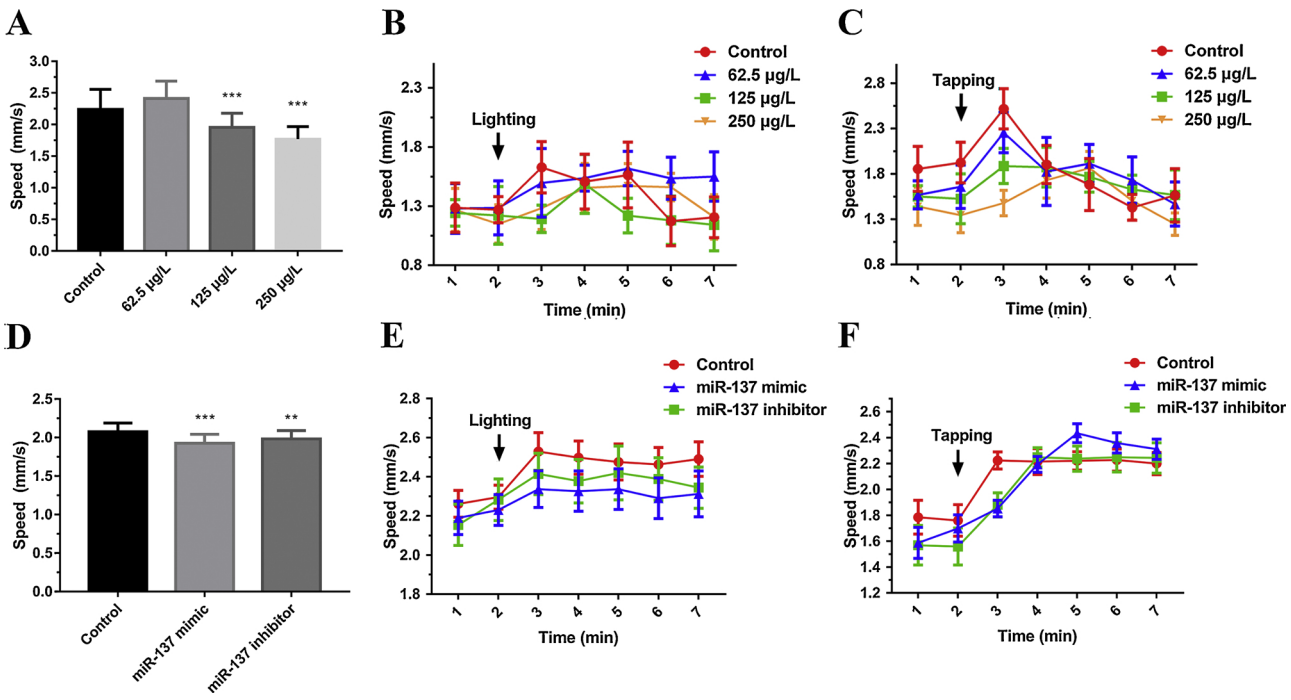

Fig. 5. Behavioral effects on 120-hpf zebrafish after TCS exposure and microinjection of miR-137. (A) Swimming speed of zebrafish larvae at 120 hpf after TCS exposure from 6 to 96 hpf; (B) Swimming speed of zebrafish larvae at 120 hpf after TCS exposure from 6 to 96 hpf when subjected to light stimulation; (C) Swimming speed of zebrafish larvae at 120 hpf after TCS exposure from 6 to 96 hpf when subjected to a tapping stimulation; (D) Swimming speed of zebrafish larvae at 120 hpf after microinjection of miR-137; (E) Swimming speed of zebrafish larvae at 120 hpf after microinjection of miR-137 when subjected to a light stimulation; (F) Swimming speed of zebrafish larvae at 120 hpf after microinjection of miR-137 when subjected to a tapping stimulation. "**" and "***" indicate significance at $p < 0.01$ and $p < 0.001$, respectively.

zebrafish brain tissue revealed ventriculomegaly (a arrow), reduced number of neurons, glial cell proliferation and formation of glial scars (b arrow) (Fig. 7A). These observations indicated the occurrence of a neuronal abnormal apoptosis phenomenon in the periglomerular gray zone (PGz). After HE staining of the adult zebrafish spinal cord, compact fiber structure and clear nucleus were observed in the control group. In contrast, TCS-exposure groups displayed a decreased number of glial cells and fiber structures became loose and hollow (Fig. 7B).

4. Discussion

Previous studies posited that miR-137 was mainly associated with neurocyte proliferation and differentiation, neurodevelopment and nervous system diseases (Li et al., 2013; Yin et al., 2014; Siegert et al., 2015). Our study demonstrated that neurotoxicity induced by TCS exposure in zebrafish resulted from upregulating miR-137 expression that suppressed neurodevelopmental related target genes and metabolic pathways. By interfering with miR-137 knockdown and overexpression, the expression of target genes was confirmed by both qRT-PCR and W-ISH. Neurotoxic effects were induced by miR-137 up-regulation and affected phenotypic malformation, neuromast development and behavioral analysis. Based on bioinformatics analysis of miRNA expression in the CNS, miR-137 was identified one of the most abundant miRNAs, but few data are available on its functions in zebrafish, although a few studies ascribe its key roles in neurocellular proliferation and differentiation in humans and mice (Li et al., 2013; He et al., 2017). Further, *miR-137* is one of the most robustly implicated genes in schizophrenia (Guan et al., 2014). It has also been linked to spinal cord injury and nervous system diseases, such as schizophrenia, post-stroke depression, Parkinson and Alzheimer (Gao et al., 2017; Zhao et al., 2013).

In this investigation, TCS exposure led to abnormal expression of miR-137 and further affected its target genes as verified by both qRT-PCR and W-ISH results. qRT-PCR demonstrated up-regulation of miR-137 from TCS exposure that led to decreased expression of its target genes, consistent with W-ISH results. These findings disclosed that TCS induced abnormal expression of miR-137 thereby affecting the normal expression of target genes. Histopathological observations revealed that miR-137 over-expression produced higher malformation rates, especially higher CNS malformations (e.g., abnormal ventricle and bent spine) in zebrafish embryos. These results implied that the most sensitive embryonic toxicological endpoint of miR-137 expression was impairment of the CNS. These malformations might be caused by the knock-down of miR-137 target genes.

This study confirmed for the first time that TCS-induced abnormal expression of miR-137 in zebrafish causes neurotoxic effects. W-ISH analysis indicated that the expression patterns of miR-137 and its target genes were mainly associated with the CNS. Given the paucity of information regarding neurotoxicity of miR-137 in zebrafish, this study provides important new information to assess various regulatory mechanisms. *Runx1*, as a target gene of miR-137, can affect cell proliferation and neuronal differentiation in adult mice neurosphere cultures (Logan et al., 2015). *bcl11aa*, as a member of the bcl family, plays an important role in cell proliferation and anti-apoptosis aspects (Chen et al., 2009). Neuronal apoptosis is a vital mechanism responsible for nervous system damage. The decreased neuromasts in stained hair cells of TCS treatments may result from hair cell apoptosis. In HE staining of adult zebrafish brain, glial cell proliferation in the 125 and 250 μg /L TCS treatments might result from decreased expression of the *runx1* or *bcl11aa* genes, which further inhibit normal cell apoptosis. MAPKs are involved in directing cellular responses to a diverse array of stimuli, such as mitogens, osmotic stress, heat shock and proinflammatory cytokines. Further, MAPKs regulate cell functions including proliferation, gene expression, differentiation, mitosis, cell survival, and apoptosis (Hoeflich et al., 2006). mmu-miR-137 is mainly associated with the MAPK signaling pathway in mice, and the MAPK signaling pathway has been reported to play an important role in pathogenesis of neurodegenerative diseases, such as Alzheimer and Parkinson (Taylor et al., 2013; Sabio and Davis, 2014). When miR-137 was over-expressed,

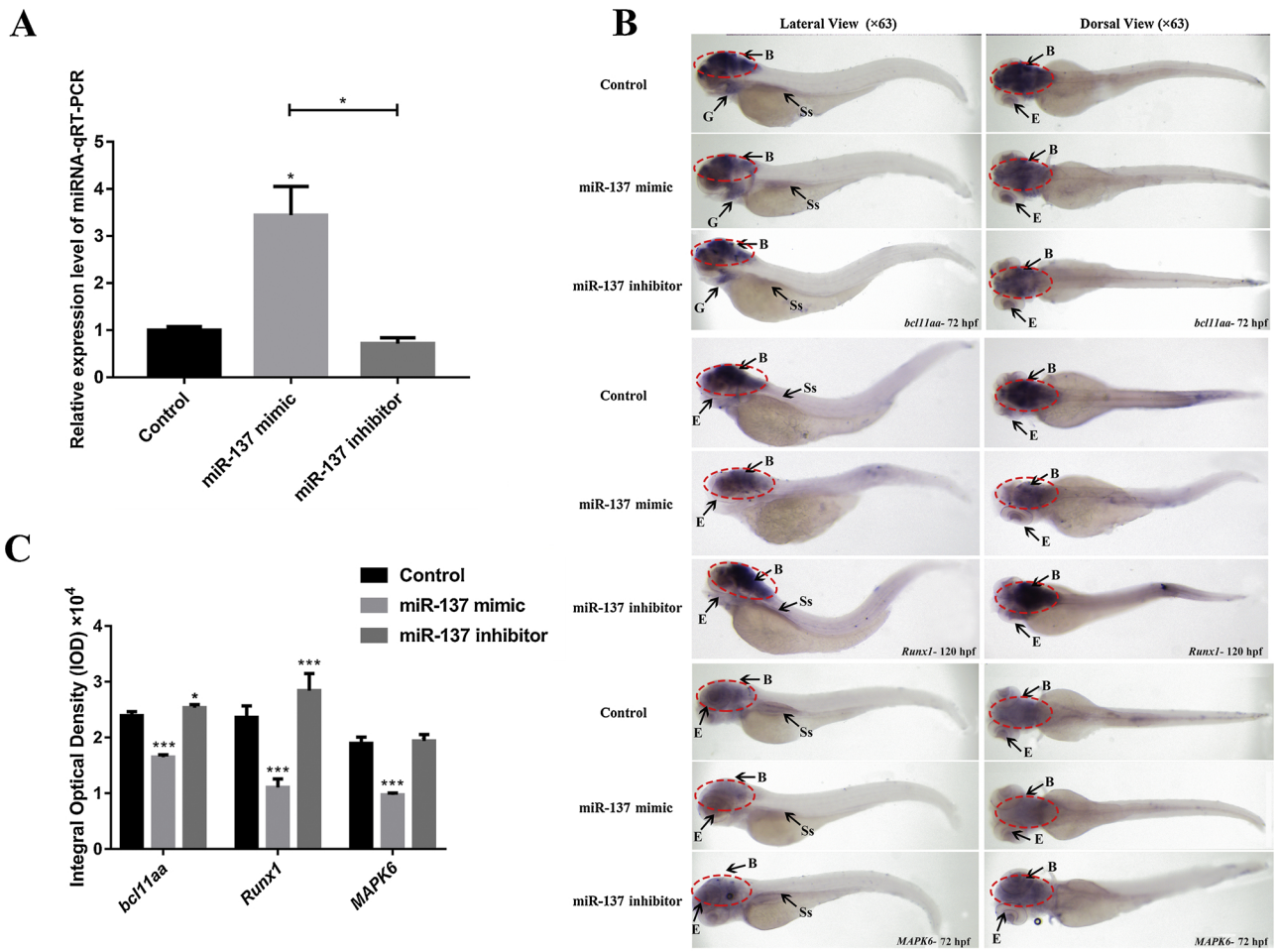

Fig. 6. The differential expression of miR-137 and miR-137 target and regulatory genes after microinjection as determined by qRT-PCR and W-ISH. (A) Differential expression of miR-137 after microinjection of miR-137 by qRT-PCR; (B) W-ISH of miR-137 target and regulatory genes after microinjection in 72 or 120-hpf larvae; (C) The IOD analysis of miR-137 target and regulatory genes. IOD analysis on whole zebrafish; Fig. 6B shows the expression of hybridization signals by lateral and dorsal view in control and treatment groups; Abbreviations in Fig. 6B: B, brain; E, eye; G, gills; SS, swimming sac; "*", and "***" indicate significance at $p < 0.05$ and $p < 0.001$.

MAPK6 expression decreased, which affected the MAPK signaling pathway, further resulting in neurotoxicity in zebrafish.

Informed by the above results, we rigorously studied the regulation and interaction of miR-137 expression with respect to TCS exposure in zebrafish. In 120 ~ 144-hpf zebrafish, the development of hair cells in the lateral-line neuromast was most intense. During the period when the lateral-line development-related genes or interfering factors were regulated, the development and differentiation of hair cells in the lateral-line neuromast might be most strongly affected. Hair cells in lateral-line neuromast are similar to human inner ear hair cells in structure and function, and thus they can be used to evaluate the ototoxicity of drugs. Based on neuromast staining, the number of neuromasts in the pLL decreased in the 250 μg/L TCS treatment suggesting that high-level TCS exposure can lead to ototoxicity in zebrafish. Ear function in zebrafish was mainly revealed by behavioral analysis; zebrafish took longer to respond to sound stimulation after high-level TCS exposure. For 120-hpf zebrafish in the over-expressed miR-137 group, the number of neuromasts in the pLL was also decreased, demonstrating that TCS affected the development of hair cells by up-regulating miR-137 expression.

Locomotive behavior in vertebrates, such as swimming, relies on neural networks in the brain and spinal cord. Drugs can affect the vitality of motor functions by impacting the nervous system, and thus locomotor activity is an important index for detecting nerve injury. As compared to the control group, the 250 μg/L TCS-exposure group led to lower locomotor activity comparable to the miR-137 over-expression group. Light stimulation tests indicated that TCS might up-regulate miR-137 through disturbing target gene expression, further resulting in impairment of sensory and motor conduction functions. These findings provide guidance for understanding the neurotoxic effect of chronic TCS exposure by inducing abnormal expression of miR-137 and its related target genes. Overall, the results of this study highlight the application of zebrafish as a vertebrate model organism for investigating the relationship between pharmaceutical exposure (and other environmental toxicants) and nervous system diseases, such as Parkinson and schizophrenia.

5. Conclusions

This study identified an important neurotoxic target, miR-137, which was highly responsive to TCS exposure. Significant miR-137 upregulation following TCS exposure induced zebrafish neurotoxicity, abnormal development of sensory organs, and visual and auditory disorders. miR-137 was demonstrated to affect the CNS through its effects on target and regulatory genes (*bcl11aa*, *Runx1* and *MAPK6*), which showed an inverse expression pattern with that of miR-137 upon TCS exposure. The most sensitive larval toxicological endpoint identified by intervened miR-137 abnormal expression was impairment of the CNS. The most notable impairments were ventricular abnormalities and curvature of the notochord. Behavioral observations demonstrated that

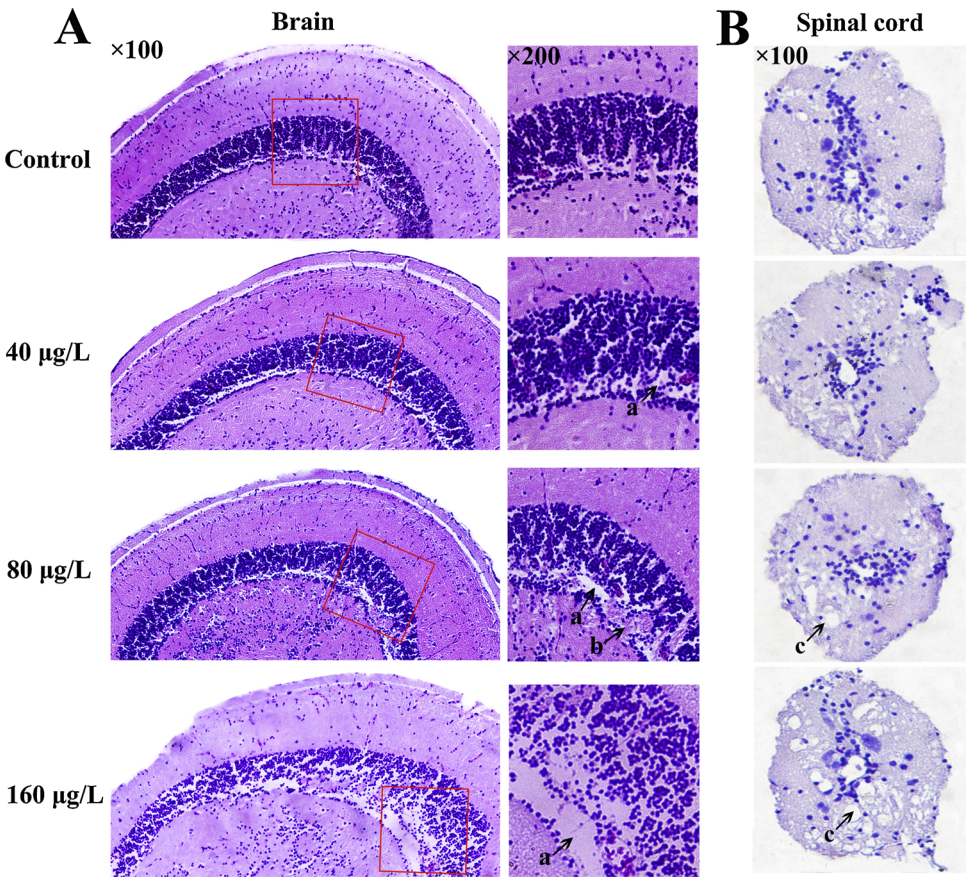

Fig. 7. Histopathological observations on 90-dpf adult zebrafish brain and spinal cord by HE staining. (A) HE staining of adult zebrafish brain; (B) HE staining of adult zebrafish spinal cord. "a arrow" in Fig. 7A shows ventriculomegaly; "b arrow" in Fig. 7A shows glial cell proliferation and formation of glial scar; "c arrow" in Fig. 7B shows bulb-like degeneration of nerve fiber.".

both TCS exposure and miR-137 over-expression led to a similar decreased in hearing and vision sensitivity due to impairment of the CNS. This study provides important mechanistic information concerning TCS-induced toxicological impacts on zebrafish. These observations provide theoretical guidance for development of early intervention treatments for nervous system diseases.

Acknowledgements

This work was jointly supported by the National Natural Science Foundation of China (31770552), the Natural Science Foundation of Zhejiang Province (LY17H26004), and the Jiangsu Provincial College Students' Innovation and Pioneering Training Project (201810332016Z).

Appendix A. Supplementary data

Supplementary material related to this article can be found, in the online version, at doi:https://doi.org/10.1016/j.aquatox.2018.11.017.

References

Carthew, R.W., Sontheimer, E.J., 2009. Origins and mechanisms of miRNAs and siRNAs. Cell 136, 642–655.
Chen, Z., Luo, H.Y., Steinberg, M.H., Chui, D.H., 2009. *BCL11A* represses HBG transcription in K562 cells. Blood Cells Mol. Dis. 42, 144–149.
Cherednichenko, G., Zhang, R., Bannister, R.A., Timofeyev, V., Li, N., Fritsch, E.B., Feng, W., Barrientos, G.C., Schebb, N.H., Hammock, B.D., 2012. Triclosan impairs excitation-contraction coupling and Ca^{2+} dynamics in striated muscle. Proc. Natl. Acad. Sci. U. S. A. 109, 14158–14165.
Damblychaudière, C., Sapède, D., Soubiran, F., Decorde, K., Gompel, N., Ghysen, A., 2003. The lateral line of zebrafish: a model system for the analysis of morphogenesis and neural development in vertebrates. Biol. Cell 95, 579–587.
Eberle, F.C., Salaverria, I., Steidl, C., Summers Jr., T.A., Pittaluga, S., Neriah, S.B., Rodriguezcanales, J., Xi, L., Ylaya, K., Liewehr, D., 2011. Gray zone lymphoma: chromosomal aberrations with immunophenotypic and clinical correlations. Mod. Pathol. 24, 1586–1597.
Friedrich, R.W., 2013. Neuronal computations in the olfactory system of zebrafish. Annu. Rev. Neurosci. 36, 383–402.
Gao, L., Dai, C., Feng, Z., Zhang, L., Zhang, Z., 2017. MiR-137 inhibited inflammatory response and apoptosis after spinal cord injury via targeting of MK2. J. Cell. Biochem. 119, 3280–3292.
Guan, F., Zhang, B., Yan, T., Li, L., Liu, F., Li, T., Feng, Z., Zhang, B., Liu, X., Li, S., 2014. MIR137 gene and target gene CACNA1C of miR-137 contribute to schizophrenia susceptibility in Han Chinese. Schizophr. Res. 152, 97–104.
Hamilton, C.K., Navarro-Martin, L., Neufeld, M., Basak, A., Trudeau, V.L., 2014. Early expression of aromatase and the membrane estrogen receptor GPER in neuromasts reveals a role for estrogens in the development of the frog lateral line system. Gen. Comp. Endocrinol. 205, 242–250.
He, D., Wu, H., Ding, L., Li, Y., 2014. Combination of BCL11A siRNA with vincristine increases the apoptosis of SUDHL6 cells. Eur. J. Med. Res. 19 34-34.
He, D., Tan, J., Zhang, J., 2017. miR-137 attenuates Aβ-induced neurotoxicity through inactivation of NF-κB pathway by targeting TNFAIP1 in Neuro2a cells. Biochem. Biophy. Res. Commun. 490, 941–947.
Hoeflich, K.P., Eby, M.T., Forrest, W.F., Gray, D.C., Tien, J.Y., Stern, H.M., Murray, L.J., Davis, D.P., Modrusan, Z., Seshagiri, S., 2006. Regulation of ERK3/MAPK6 expression by BRAF. Int. J. Oncol. 29, 839–849.
Huang, D.W., Sherman, B.T., Lempicki, R.A., 2009. Bioinformatics enrichment tools: paths toward the comprehensive functional analysis of large gene lists. Nucleic Acids Res. 37, 1–13.
Jackson-Browne, M.S., Papandonatos, G.D., Chen, A., Calafat, A.M., Yolton, K., Lanphear, B.P., Braun, J.M., 2018. Identifying vulnerable periods of neurotoxicity to triclosan exposure in children. Environ. Health. Persp. 126, 1–9.
Jia, X., Wang, F., Han, Y., Geng, X., Li, M., Shi, Y., Lu, L., Chen, Y., 2016. miR-137 and miR-491 negatively regulate dopamine transporter expression and function in neural cells. Neurosci. Bull. 32, 1–11.
Kloosterman, W.P., Wienholds, E., de Bruijn, E., Kauppinen, S., Plasterk, R.H., 2006. In situ detection of miRNAs in animal embryos using LNA-modified oligonucleotide probes. Nat. Methods 3, 27–29.
Krol, J., Loedige, I., Filipowicz, W., 2010. The widespread regulation of microRNA biogenesis, function and decay. Nat. Rev. Genet. 11, 597–610.
Kyung, P.B., Gonzales, E.L.T., Yang, S.M., Bang, M., Soon, C.C., Young, S.C., 2016. Effects of triclosan on neural stem cell viability and survival. Biomol. Ther. (Seoul) 24, 99–107.
Lassen, T.H., Frederiksen, H., Kyhl, H.B., Swan, S.H., Main, K.M., Andersson, A.M., Lind, D.V., Husby, S., Wohlfahrt-Veje, C., Skakkebæk, N.E., 2016. Prenatal triclosan exposure and anthropometric measures including anogenital distance in Danish infants. Environ. Health Perspect. 124, 1261–1268.
Li, K.W., Yang, L., Pang, C.S., Chan, K.Y., Zhou, L., Mao, Y., Wang, Y., Lau, K.M., Poon, W.S., Shi, Z., 2013. MIR-137 Suppresses growth and invasion is downregulated in

oligodendroglial tumors and targets CSE1L. Brain Pathol. 23, 426–439.
Logan, T.T., Rusnak, M., Symes, A.J., 2015. Runx1 promotes proliferation and neuronal differentiation in adult mouse neurosphere cultures. Stem Cell Res. 15, 554–564.
Meador, J.P., Yeh, A., Gallagher, E.P., 2018. Adverse metabolic effects in fish exposed to contaminants of emerging concern in the field and laboratory. Environ. Pollut. 236, 850–861.
Mitsuda, Y., Morita, K., Kashiwazaki, G., Taniguchi, J., Bando, T., Obara, M., Hirata, M., Kataoka, T.R., Muto, M., Kaneda, Y., 2018. *RUNX1* positively regulates the ErbB2/HER2 signaling pathway through modulating SOS1 expression in gastric cancer cells. Sci. Rep. 8, 6423.
Mufson, E.J., He, B., Nadeem, M., Perez, S.E., Counts, S.E., Leurgans, S., Fritz, S., Lah, J., Ginsberg, S.D., Wuu, J., Scheff, S.W., 2012. Hippocampal proNGF signaling pathways and β-amyloid levels in mild cognitive impairment and Alzheimer disease. J. Neuropathol. Exp. Neurol. 71, 1018–1029.
Muth-Köhne, E., Wichmann, A., Delov, V., Fenske, M., 2012. The classification of motor neuron defects in the zebrafish embryo toxicity test (ZFET) as an animal alternative approach to assess developmental neurotoxicity. Neurotoxicol. Teratol. 34, 413–424.
Oliveira, R., Domingues, I., Koppe Grisolia, C., Soares, A.M., 2009. Effects of triclosan on zebrafish early-life stages and adults. Environ. Sci. Pollut. Res. Int. 16, 679–688.
Philippat, C., Botton, J., Calafat, A.M., Ye, X., Charles, M.A., Slama, R., 2014. Prenatal exposure to phenols and growth in boys. Epidemiology 25, 625–635.
Popova, L.B., Nosikova, E.S., Kotova, E.A., Tarasova, E.O., Nazarov, P.A., Khailova, L.S., Balezina, O.P., Antonenko, Y.N., 2018. Protonophoric action of triclosan causes calcium efflux from mitochondria, plasma membrane depolarization and bursts of miniature end-plate potentials. BBA-Mol. Basis. Dis. 1860, 1000–1007.
Ruszkiewicz, J.A., Li, S., Rodriguez, M.B., Aschner, M., 2017. Is triclosan a neurotoxic agent? J. Toxicol. Environ. Health B 20, 104–117.
Sabio, G., Davis, R.J., 2014. TNF and MAP kinase signaling pathways. Semin. Immunol. 26, 237–245.
Siegert, S., Seo, J., Kwon, E.J., Rudenko, A., Cho, S., Wang, W., Flood, Z., Martorell, A.J., Ericsson, M., Mungenast, A.E., 2015. The schizophrenia risk gene product miR-137 alters presynaptic plasticity. Nat. Neurosci. 18, 1008–1016.
Szychowski, K.A., Wnuk, A., Kajta, M., Wójtowicz, A.K., 2016. Triclosan activates aryl hydrocarbon receptor (AhR)-dependent apoptosis and affects Cyp1a1 and Cyp1b1 expression in mouse neocortical neurons. Environ. Res. 151, 106–114.
Taylor, D.M., Moser, R., Régulier, E., Breuillaud, L., Dixon, M., Beesen, A.A., Elliston, L., Santos, M.D.F.S., Kim, J., Jones, L., 2013. MAP kinase phosphatase 1 (MKP-1/DUSP1) is neuroprotective in Huntington's disease via additive effects of JNK and p38 inhibition. J. Neurosci. 33, 2313–2325.
Thisse, C., Thisse, B., 2008. High-resolution in situ hybridization to whole-mount zebrafish embryos. Nat. Protoc. 3, 59–69.
Van, T.D.M., Artachocordón, F., Swaab, D.F., Struik, D., Makris, K.C., Wolffenbuttel, B., Frederiksen, H., Van, V.O., 2017. Distribution of non-persistent endocrine disruptors in two different regions of the human brain. Int. J. Environ. Res. Public Health 14, e1059.
Veena, S.R., Krishnaveni, G.V., Wills, A.K., Kurpad, A.V., Muthayya, S., Hill, J.C., Karat, S.C., Nagarajaiah, K.K., Fall, C.H.D., Srinivasan, K., 2010. Association of birthweight and head circumference at birth to cognitive performance in 9- to 10-year-old children in south India: prospective birth cohort study. Pediatr. Res. 67, 424–429.
Wang, C.F., Tian, Y., 2015. Reproductive endocrine-disrupting effects of triclosan: population exposure, present evidence and potential mechanisms. Environ. Pollut. 206, 195–201.
Weatherly, L.M., Nelson, A.J., Shim, J., Riitano, A.M., Gerson, E.D., Hart, A.J., Juan-Sanz, J.D., Ryan, T.A., Sher, R., Hess, S.T., 2018. Antimicrobial agent triclosan disrupts mitochondrial structure, revealed by super-resolution microscopy, and inhibits mast cell signaling via calcium modulation. Toxicol. Appl. Pharm. 349, 39–54.
Weilin, L., Shelver, Lisa M., Kamp, Jennifer L., Church, Rubio, F.M., 2007. Measurement of Triclosan in water using a magnetic particle enzyme immunoassay. J. Agric. Food. Chem. 55, 3758–3763.
Westerfield, M., 2000. The Zebrafish Book. A Guide for the Laboratory Use of Zebrafish (*Danio Rerio*). Univ. of Oregon Press, Eugene, OR, USA.
Wienholds, E., Kloosterman, W.P., Miska, E., Alvarezsaavedra, E., Berezikov, E., de Bruijn, E., Horvitz, H.R., Kauppinen, S., Plasterk, R.H., 2005. MicroRNA expression in zebrafish embryonic development. Science 309, 310–311.
Xu, B., Zhang, Y., Du, X.F., Li, J., Zi, H.X., Bu, J.W., Yan, Y., Han, H., Du, J.L., 2017. Neurons secrete miR-132-containing exosomes to regulate brain vascular integrity. Cell. Res. 27, 882–897.
Yin, J., Lin, J., Luo, X., Chen, Y., Li, Z., Ma, G., Li, K., 2014. miR-137: a new player in schizophrenia. Int. J. Mol. Sci. 15, 3262–3271.
Ying, G.G., Kookana, R.S., 2007. Triclosan in wastewaters and biosolids from Australian wastewater treatment plants. Environ. Int. 33, 199–205.
Yu, A.M., Pan, Y.Z., 2012. Noncoding microRNAs: small RNAs play a big role in regulation of ADME? Acta Pharm. Sin. B 2, 93–101.
Zhang, Y., Liu, M., Liu, J., Wang, X., Wang, C., Ai, W., Chen, S., Wang, H., 2018. Combined toxicity of triclosan, 2,4-dichlorophenol and 2,4,6-trichlorophenol to zebrafish (*Danio rerio*). Environ. Toxicol. Pharmacol. 57, 9–18.
Zhao, L., Li, H., Guo, R., Ma, T., Hou, R., Ma, X., Du, Y., 2013. miR-137, a new target for post-stroke depression? Neural Regen. Res. 8, 2441–2448.